

Research Article

## Antibacterial potential of bacterial cellulose composite with levofloxacin against pathogens from wounds and burns infections in Basrah, Iraq

Fatima Salem Al-halfi

Department of Biology, College of Science, University of Basrah, Basrah, Iraq

Wijdan Hussein Al-Tamimi \* 

Department of Biology, College of Science, University of Basrah, Basrah, Iraq

\*Corresponding author. E-mail: wijdan.abdulsahib@uobasrah.edu.iq

### Article Info

<https://doi.org/10.31018/jans.v18i1.7151>

Received: September 03, 2025

Revised: March 01, 2026

Accepted: March 07, 2026

### How to Cite

Al-halfi, F.S. and Al-Tamimi, W.H. (2026). Antibacterial potential of bacterial cellulose composite with levofloxacin against pathogens from wounds and burns infections in Basrah, Iraq. *Journal of Applied and Natural Science*, 18(1), 511 - 526. <https://doi.org/10.31018/jans.v18i1.7151>

### Abstract

Bacterial cellulose (BC) has attracted attention as a drug delivery platform due to its structural strength and biocompatibility. In the present study, BC produced by *Bacillus licheniformis* was tested against bacteria isolated from wound and burn infections. BC was fabricated in situ with gellan and whey Bacterial cellulose/gellan gum (BC/GW) and ex situ with sodium alginate and levofloxacin at different concentrations Bacterial cellulose/gellan gum/ levofloxacin (BC/GW/SA/LEV) to improve its antibacterial efficacy. Molecular detection using the 16S rRNA gene was employed to identify 31 bacterial isolates. The BC films were characterized by measuring water-holding capacity (WHC), Fourier transform infrared (FTIR), Scanning electron microscopy (SEM), and Thermal gravimetric analysis (TGA). The results indicated that the most prevalent genera were *Staphylococcus* sp. 13 (52%) and *Escherichia* sp. 4 (16%). In terms of frequency, *Staphylococcus aureus* was the most common species, found in 6 isolates (20%). The isolate of *Bacillus licheniformis* demonstrated a high BC yield of 188 g/l, which increased to 289 g/l after in situ fabrication. The BC/GW film exhibited the highest WHC improvement at 96.03%, compared to the BC film at 93.93%. FTIR confirmed successful bonding between the BC/GW/SA/LEV film and levofloxacin. TGA analysis showed moderate thermal stability for the BC film and BC/GW, whereas BC/GW/SA exhibited significantly enhanced thermal stability. SEM revealed a three-dimensional porous fibrous network of BC. The BC/GW film appeared denser and more compact. The BC/GW/SA film appeared more homogeneous, with filled voids, and the BC/GW/SA/LEV surface exhibited branched crystalline domains, indicating successful incorporation of levofloxacin. The composites exhibited strong antibacterial activity, with a maximum inhibition zone of 35 mm for *Bacillus bacterium* strain ZHCPRcN32 at a concentration of 7.5 mg, and the lowest was against *Escherichia coli* at 11 mm at the same concentration. The BC composite films may play a promising role in treating multidrug-resistant wound infections by serving as carriers for antibiotics targeting these bacteria.

**Keywords:** Antibacterial activity, Bacterial cellulose, Composite fabrication, Levofloxacin, Wound infections

### INTRODUCTION

Chronic wounds are ulcers that do not heal and are often associated with bacterial infections. Because of compromised cellular responses and increased inflammation, which are probably brought on by bacterial infection and biofilm formation, these wounds evade the natural healing process (Chamoun and Matheus, 2025). Wound infections remain an interprofessional and interdisciplinary challenge, particularly in patients with chronic wounds (Dissemond *et al.*, 2025). In daily clinical practice, multidrug-resistant organisms (MDROs) present a significant challenge. This term

describes a group of bacteria that exhibit strong antibiotic resistance. Approximately 1.2 million individuals worldwide die each year as a result of antibiotic resistance (Murray *et al.*, 2022). Gram-positive cocci (*Staphylococcus aureus* and *Enterococcus faecalis*) and gram-negative bacilli (*Pseudomonas aeruginosa* and *Klebsiella pneumoniae*) dominate wound infections (Bhujugade *et al.*, 2024). Even though there are numerous therapeutic approaches for treating wounds and burns, and significant advancements have been made in this field, there is still an opportunity for improvement because better ways to hasten wound healing and recovery are desperately needed, particularly for patients

who have suffered severe burns. Bacterial cellulose (BC), produced by bacteria, offer several benefits over vegetable cellulose. BC can be modified to confer antibacterial activity and potential local drug-delivery properties (Portela *et al.*, 2019). The exceptional properties of BC materials include high surface area and high crystallinity (84.89%). It has superior mechanical qualities and is more compatible with the degree of polymerization. BC differs from other cellulose polymers due to its high water-holding capacity. This is because the absence of lignin and hemicellulose results in a high degree of purity. Considered highly biocompatible, non-cytotoxic, and non-genotoxic, it is the most effective material now used to heal complex wounds. The moist environment that the BC dressing provides, enhance the dressing's capacity to retain moisture making application easier and resulting in a longer wear period that is more cost-effective (Sulaeva *et al.*, 2020). Numerous bacteria from the genera *Acetobacter*, *Achromobacter*, *Komagatasibacter*, *Agrobacterium*, *Bacillus*, *Azotobacter*, *Sarcinia*, *Lactobacillus*, and *Gluconacetobacter* produce BC (Avcioglu, 2022). Another popular area of study is the modification of BC to enhance its functionality (Cazón and Vázquez, 2021). In situ modification is a desirable alteration technique that involves both fermentation and the simultaneous performance of BC modification with additives (Stumpf *et al.*, 2018). Chemical modification, enzymatic methods, and genetic engineering can maximize the performance of BC. To date, numerous reviews have addressed the optimization and modification of BC-based composites (Ullah *et al.*, 2024). The creation of antimicrobial scaffolds that combat bacteria and fungi utilizes a variety of materials, including glass, ceramics, biopolymers, polymers, and antimicrobial compounds such as peptides, antibiotics, and antiseptics, as well as combinatorial techniques, metals, and carbon nanomaterials (Serrano-Aroca *et al.*, 2022). Over the past ten years, researchers have focused on enhancing the benefits and uses of BC through a variety of strategies (Malcı *et al.*, 2024). Most of the bacteria that produced BC were isolated from natural sources. The present study aimed to produce BC from selected bacteria isolated from harsh environments, *Bacillus licheniformis* obtained from oil reserves in Iraq, to develop a novel drug delivery composite that inhibits the growth of pathogens and is suitable for use as a wound dressing

## MATERIALS AND METHODS

### Samples collection and culturing of bacteria

Thirty-two clinical samples were collected from patients with contaminated burns and wounds at Al-Sadr Teaching Hospital in Basrah Governorate, Iraq, from May to July 2025. Samples were taken using sterile gel swabs and, immediately transported to the laboratory for fur-

ther microbiological analysis. All collected samples were cultured on blood agar and MacConkey agar plates, incubated at 37 °C for 24 hrs. The distinct colonies were subcultured onto nutrient agar three times to ensure their purity. A microscopic investigation was conducted using the Gram stain procedure.

### Genetic identification and sequencing of bacterial isolates

Genomic DNA was extracted from all bacterial isolates using the Geneaid Bacteriology Kit (Geneaid, USA), according to the manufacturer's protocol. To amplify the 16S rRNA gene, polymerase chain reaction (PCR) was performed using the universal forward primer 27F (5' AGAGTTTGATCCTGGCTCAG-3') and the reverse primer 1492R (5' GGTTACCTTGTTACGACTT-3'). The PCR mixture contained primer solution prepared according to the manufacturer's instructions; the reaction mixture was made with the AccuPower® PCR PreMix kit. The thermal cycle program was as follows: initial denaturation for 4 min at 96°C, followed by 28 cycles of denaturation at 94°C for 30 s, annealing at 56°C for 45 s, extension at 72°C for 2 min, and a final elongation step at 72°C for 10 min. PCR products were electrophoresed on a 1.5 % (w/v) agarose gel using a 100-bp DNA ladder at 70 V and 120 mA for 60 min. The PCR-generated 16S rRNA gene fragments were purified by MacroGen (South Korea) for sequencing using the same primers. The 16S rRNA gene sequences were compared with the nucleotide sequences in NCBI using the BLAST program (<http://www.ncbi.nlm.nih.gov/BLAST>). The neighbor-joining method of phylogenetic analysis was used to infer evolutionary relationships among the examined taxa. Bootstrap analysis was used to assess the inferred tree's robustness using 1000 replicates; only branches with bootstrap values greater than 50% are displayed. The amount of nucleotide changes per site was used to compute evolutionary distances using the p-distance method. Twenty-five nucleotide sequences were included in the analysis. The total deletion option was used to eliminate all sites with gaps or missing data, leaving a final dataset with 754 aligned nucleotide positions. MEGA version 11 was used to create and analyze phylogenetic trees (Tamura *et al.*, 2021).

### Production and extraction of bacterial cellulose (BC) by *Bacillus licheniformis*

*B. licheniformis* was provided by the Applied Microbiology Laboratory, Department of Biology, College of Science, University of Basrah. The primary (seed) inoculum was prepared by growing *B. licheniformis* on agar, excising a 24 h-old culture, and transferring it aseptically with sterile forceps into 50 ml of nutrient broth in a 100 ml flask. The culture was incubated at 35 °C for 24 hrs. under shaking conditions. Subsequently, 10% (v/v)

of the activated inoculum (approximately  $10^6$ – $10^7$  CFU/ml) was used to inoculate 100 ml of BC production modified Hestrin and Schramm (MHS) medium in 250 ml Erlenmeyer flasks, consisting of g/l: 50 g glucose, 5 g yeast extract, and 12 g  $\text{CaCO}_3$ . The medium pH was adjusted to 5.5 with 1 M NaOH. The flasks were incubated under static conditions at 35°C for 14 days (Orlando *et al.*, 2020). After incubation, the surface layer was separated from the production medium and subjected to a series of purification steps. Initially, it was rinsed repeatedly with distilled water to remove any residual components of the culture medium. Subsequently, the layer was treated with 1% (w/v) NaOH for 10 min. Then, the layer was washed multiple times with distilled water to ensure complete elimination of any remaining alkaline residues, dried at room temperature, and autoclaved to eliminate residual bacteria and spores (Atta *et al.*, 2021).

#### **In situ and ex situ fabrication of bacterial cellulose (BC)**

To create a drug-loaded composite meant for use as a dressing, BC was combined with gellan and sodium alginate, and then levofloxacin was added. First the BC/GW (bacterial cellulose/gellan whey) was fabricated in situ by combining 50 ml of whey with 50 ml of the modified Hestrin and Schramm medium supplemented with 0.04 g (w/v) of  $\text{FeCl}_3$  and 0.025 g (w/v) of gellan gum. For ex situ fabrication, the BC/GW/SA/LEV composites (bacterial cellulose/gellan whey/sodium alginate/Levofloxacin) were prepared according to Saleh *et al.* (2022), with some modifications using solution mixing and pouring methods. Initially, 50 g of wet BC was cut into small pieces and homogenized in 100 mL of deionized water ( $\text{dH}_2\text{O}$ ) using a hand mixer for 10 min to obtain a homogeneous BC fibre suspension. Sodium alginate (SA) was separately dissolved in  $\text{dH}_2\text{O}$  at a concentration of 2 % (w/v) to form a viscous solution. The SA solution was then mixed with the BC suspension at a volume ratio, with continuous stirring to ensure homogeneity. For drug delivery, different concentrations of Levofloxacin (LEV) (7.5, 5.0, 2.5, 1.0, 0.5, and 0.1 mg) were added to 25 ml of the BC/SA mixture, along with a few drops of glycerol. The resulting mixtures were homogenized ultrasonically for 5 min in an ice-cold water bath to prevent thermal decomposition. Finally, each mixture was poured into 6 cm petri dishes and dried in an oven at 35°C for 48 hrs. The formed films were carefully removed and stored in a vacuum desiccator until use. Control films (BC/GW/SA without LEV) were prepared under similar conditions.

#### **Characterization of BC films**

The water-holding capacity (WHC) of BC films was determined according to (Machado *et al.*, 2016). The Fourier transform infrared spectroscopy (FTIR) was con-

ducted using an FTIR spectrometer (FTIR alpha II / Germany, Bruker). The spectra were recorded in transmittance mode in the range of 4,000–400  $\text{cm}^{-1}$ . The MIRA3 scanning electron microscopy (SEM) at Shiraz University in Iran was used to evaluate the surface morphology of BC, BC/GW, and BC/GW/SA/LEV films. Samples were analyzed at an accelerating voltage of 20 kV after being thinly coated with gold by sputtering. At Taban Lab in Tehran, Iran, thermogravimetric analysis (TGA) was performed using an SDT Q600 V20.9 (DSC-TGA) thermogravimetric analyzer. About  $2.655 \pm 1$  mg of dried samples were heated under a continuous argon flow (40 ml/min) from 24°C to 1008.61°C at a steady rate of 20°C/min.

#### **Antimicrobial activity of composite film BC/GW/SA/LEV**

The composite film of BC/GW/SA/LEV, fabricated with a specific antimicrobial agent, was tested against several isolates of burn and wound infections. Testing was conducted using the disc diffusion method. Composite film pieces (5 mm × 4 mm) were placed on Mueller-Hinton agar plates inoculated with 100  $\mu\text{l}$  of activated bacterial suspension ( $10^8$  CFU/ml). BC/GW/SA/LEV films containing varying concentrations of LEV were applied to the agar and incubated for an additional 24 hrs. at 37°C. Antibacterial activity was assessed by measuring the diameter of the inhibition zone around each sample. An LEV-free BC/GW/SA film served as the control.

#### **Statistical analysis**

Every experiment was carried out in triplicate as separate biological replicates, including assays for antibacterial activity, BC production, and WHC determination. Results are presented as the mean  $\pm$  standard deviation (SD) of three experiments. Statistical significance was determined using ANOVA, the T-Test, and Duncan's multiple comparison test and analyzed with SPSS version 26 (2019).

## **RESULTS AND DISCUSSION**

#### **Isolation and genetic identification of bacteria**

This study investigated the prevalence and diversity of pathogenic bacteria responsible for infections in wounds and burns. The results showed that only 23 out of 32 samples exhibited bacterial growth. A total of 31 isolates were obtained, Gram-positive isolates outnumbering Gram-negative at 26 (83.87%) compared to 5 (16.13%). This finding aligns with previous research indicating that Gram-positive bacteria, including *Staphylococcus aureus* and *Enterococcus* sp., are the predominant early colonizers in wounds. These bacteria are part of the normal skin flora and quickly invade underlying tissue upon disruption of the skin barrier, mak-

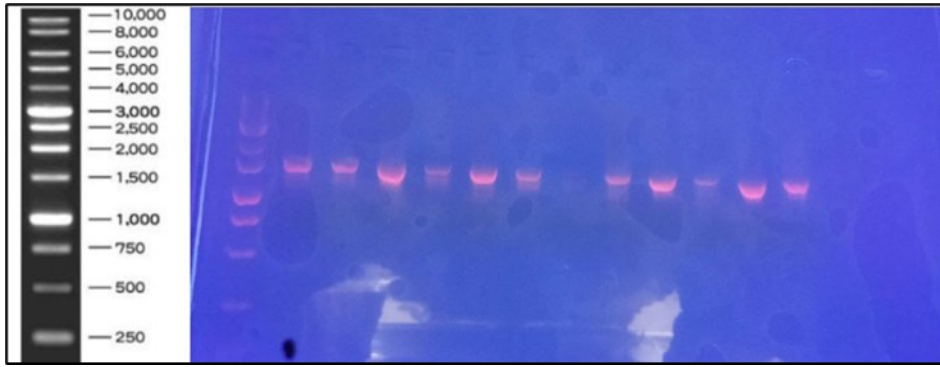


**Fig.1.** Polymerase chain reaction-amplified products of the 16S rRNA gene for bacterial isolates

ing them key agents in early-stage wound infections (Devi *et al.*, 2024). Gram-negative bacteria colonize wounds later, especially in chronic or hospital-acquired infections, and dominate after the second week post-injury, while Gram-positive cocci are prevalent during the first 7-10 days (Devi *et al.*, 2024). Thirty-one isolates that proceeded with 16S rRNA sequencing had pure and clear extracted DNA, and a single amplification of about 1500 bp for all isolates was obtained (Fig. 1). This study's amplified 16S rRNA gene fragment (~1500 bp) is in line with other studies that described the molecular identification of different bacterial species isolated from clinical samples, oil-contaminated soils and water and petroleum reservoirs. (Hamzah *et al.*, 2020; Aboud *et al.*, 2021; Alyousif *et al.*, 2022; AL-Zaidi *et al.*, 2023; AL-Shami *et al.*, 2023; AL-assdy *et al.*, 2025; Hamel *et al.*, 2026).

Only 25 isolates showed successful sequencing. A BLASTn analysis of 16S rRNA gene sequences from these isolates showed that the isolates belong to eight genera and 15 species, as indicated in (Table 1). These genera included *Staphylococcus* sp., *Corynebacterium* sp., *Enterobacter* sp., *Bacillota* sp., *Klebsiella* sp., *Escherichia* sp., *Pseudomonas* sp., and *Bacillus* sp. all isolates were identified with 100% similarity, with only six showing 99% these isolates were registered as new strains in the GenBank database under accession

numbers as shown in (Table 2). The most prevalent genera were *Staphylococcus* sp. 13 (52%), and *S. aureus* showed the superiority in frequency among other species with a percentage of 5 (20%) (Fig. 2). Numerous investigations have documented that pathogenic bacteria, namely *Staphylococcus aureus*, *Pseudomonas aeruginosa*, *Escherichia coli*, and *Klebsiella pneumoniae*, are prevalent in burn and wound infections. These bacteria were identified from burn units in Bahrain and Iraq, as well as other African countries. (Rahim Hateet, 2021; AlHawaj *et al.*, 2024; Monk *et al.*, 2024). The frequent detection of *S. aureus* in such infections can be attributed to its ability to produce a wide array of virulence factors, including biofilm formation, hemolysins ( $\alpha$ ,  $\beta$ ,  $\gamma$ ,  $\delta$ ), coagulases, and proteases (Touaitia *et al.*, 2025), as well as a thick peptidoglycan layer, enzymes, toxins, penicillinase, and hyaluronidase, which altogether enhance their survival and persistence in the wound environment (Maitz *et al.*, 2023). Similarly, the study's 16% prevalence of *Escherichia coli* is within the range of wound infection rates reported globally (MMasoud *et al.*, 2020; Alsarhan and Çam, 2023). Despite variations observed elsewhere (Chaudhary *et al.*, 2019; Rahim Hateet, 2021), *Enterobacter* sp., such as *E. hormaechei* and *E. cloacae*, accounted for 8%, consistent with findings from burn-related investigations in surrounding countries (Mosaffa *et al.*, 2024). Notably,

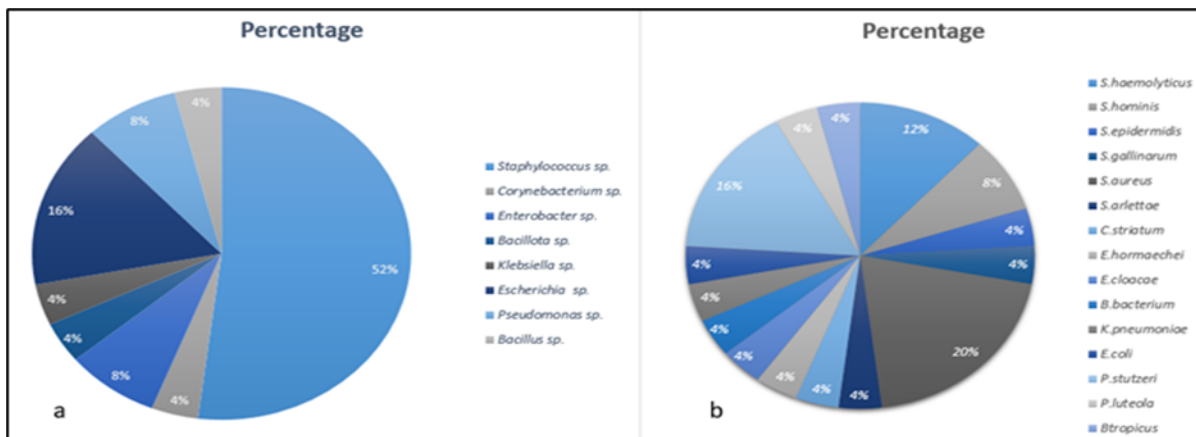


**Fig. 2.** Percentage of pathogenic bacteria isolated from wound and burn infections: a. Bacterial genera. b. Bacterial species.

**Table 1.** Genetic identification of pathogenic bacteria isolated from wound and burn infections

code	strains	Ident.%	Accession No.
A09	<i>Escherichia coli</i> strain NF73_5	100.00%	MT649839.1
A10	<i>Escherichia coli</i> strain R61	99.91%	PP593544.1
B09	<i>Pseudomonas luteola</i> strain 571	100.00%	HQ173812.1
B 10	<i>Staphylococcus hominis</i> strain BaAP2	100.00%	JQ734768.1
B11	<i>Staphylococcus aureus</i> strain IF6SW-P3A	100.00%	KY218833.1
B12	<i>Staphylococcus aureus</i> strain ABC17	100.00%	ON631076.1
C10	<i>Escherichia coli</i> strain EW1-48	99.89%	PQ591621.1
C11	<i>Staphylococcus aureus</i> strain SA05	100.00%	PP292032.1
C12	<i>Bacillus tropicus</i> strain AWMBI9	100.00%	PP564409.1
D09	<i>Pseudomonas iranica</i> strain GH10	99.81%	NR_178637.1
D10	<i>Escherichia coli</i> strain TEM 113	100.00%	MT912573.1
D11	<i>Staphylococcus haemolyticus</i> strain yasmun69	100.00%	OK632095.1
E11	<i>Klebsiella pneumoniae</i> strain M2-2-2	100.00%	MW375524.1
E 12	<i>Enterobacter cloacae</i> strain ZG606	100.00%	PQ781588.1
F09	<i>Bacillota bacterium</i> strain ZHCPRcN32	100.00%	PQ779998.1
F10	<i>Staphylococcus haemolyticus</i> strain WS1-1	100.00%	MN448415.1
F11	<i>Staphylococcus aureus</i> strain fsznc-13	100.00%	PQ269408.1
F12	<i>Staphylococcus arlettae</i> strain MSH5-2	100.00%	OM074002.1
G09	<i>Enterobacter hormaechei</i> strain Xiangfangensis LMG 27195(T)	100.00%	PQ489478.1
G10	<i>Staphylococcus aureus</i> strain SA04	99.77%	PV147266.1
G11	<i>Staphylococcus gallinarum</i> strain OOM34	99.90%	MH542297.1
G12	<i>Staphylococcus epidermidis</i> strain 45HB94_10020180_10020180,	100.00%	MT445232.1
H09	<i>Staphylococcus hominis</i> subsp. novobiosepticus strain HUC3_26b_K	99.90%	KT168275.1
H10	<i>Corynebacterium striatum</i> strain 1910ICU141	100%	MT225764.1
H11	<i>Staphylococcus haemolyticus</i> IRQBAS113	100.00%	LC647817.1

the low prevalence of *Pseudomonas aeruginosa* contrasts with many Iraqi and global reports that identify it as a dominant pathogen in burn and chronic wound infections (Rahim Hateet, 2021; Ndikubwimana *et al.*, 2024). This disparity could result from variations in antibiotic use, sample collection schedules, or infection control strategies. Low frequencies of other *Pseudomonas* sp. were found, indicating potential environmental or hospital-acquired origins (Barry, 2021). In burn settings, the prevalence of *Klebsiella pneumoniae* (4%) reported in this study falls within the broad range documented in the literature, from low rates to notably higher prevalence (Khalid *et al.*, 2024; Sun *et al.*, 2025). Overall, these comparisons show that although the results mostly reflect local epidemiology, they are generally consistent with regional and global patterns, suggesting cautious generalizability and highlighting the impact of clinical and geographic diversity on wound microbiology (Fig. 3). It illustrates a neighbour-joining

phylogenetic tree generated with MEGA 11 using 16S *rRNA* gene sequences. The branch nodes display bootstrap values (1,000 repetitions)  $\geq 50\%$ . The tree showed evolutionary relationships among closely related type strains in the GenBank database and the bacterial samples used in this investigation.

#### **Production of bacterial cellulose by *Bacillus licheniformis***

The isolate of *B. licheniformis* was tested to produce BC, a positive result was indicated by brown leather-like color, a highly flexible film with a spongy, gelatinous mat-like structure (BC pellicle) formed at the air-liquid interface after 7 days of static growth conditions, and the thickness of the film was about 2 mm (Fig. 4). This finding agrees with a previous study (Saleh *et al.*, 2022). The abundance of *Bacillus* sp. gives them an advantage over other bacteria due to greater growth rates, even on inexpensive substrates and under harsh

**Table 2.** New bacterial strains deposited in the NCBI GenBank database

New strains in GenBank	Accession No.
<i>Escherichia coli</i> strain WFatima Bas	PX021951.1
<i>Staphylococcus aureus</i> strain WFatima Bas	PX021959.1
<i>Staphylococcus gallinarum</i> strain WFatima Bas	PX021960.1
<i>Pseudomonas iranica</i> strain WFatima Bas	PX021964.1
<i>Escherichia coli</i> strain WFatima Bas25	PX021970.1
<i>Staphylococcus hominis</i> subsp. novobiosepticus strain WFatima Bas	PX021961.1

ecological conditions. So far, there are many ways to increase BC yield. One of them is isolating new bacterial strains that efficiently produce BC from nature (Aydin and Aksoy, 2014). The isolate in the present study demonstrated relatively high BC production, with wet weights of  $188.0 \pm 1.0$  g/l and dry weights of  $10.7 \pm 1.0$  g/l. These productivity levels put this isolate in a competitive position among certified BC producers. Phong *et al.* (2017) reported that *Acetobacter* sp. showed 213.87 g cellulose/300 ml of fermented mature coconut water. The *Acetobacter senegalensis* MA1 strain yielded 469.83 g/L (wet weight) after improvement (Aswini *et al.*, 2020). Compared to other strains of the same bacterial species, *Bacillus licheniformis* ZBT2 achieved a yield of 9.2 g/L (dry weight) after comprehensive improvement (Bagewadi *et al.*, 2020). The *Komagataeibacter* sp., considered the typical producer of BC, exhibits varying productivity: *Komagataeibacter xylinus* has yielded 1.6-1.9 g/l (Raiszadeh-Jahromi *et al.*, 2020), while other strains have achieved yields as high as 18.4 g/l (Bekatorou *et al.*, 2019).

After the BC surface layer was successfully isolated from the production medium, a distinct, spongy, gelatinous membrane formed. Sequential rinsing with distilled water effectively reduced residual medium components, which indicates efficient preliminary cleaning. The medium was treated with 1% (w/v) NaOH for 10 min. The treatment visibly enhanced the clarity of the cellulose sheet, reflecting the removal of cellular debris and associated impurities. Final washes with distilled water yielded a neutral pH, confirming the complete elimination of alkaline residues (Fig. 4).

#### In Situ fabrication of BC/GW

In the present study, BC was produced using an MHS medium supplemented with glucose, as this is considered the main source of BC production. Since it is a precursor for cellulose synthesis, all compounds that can be transformed into glucose are capable of forming BC (Parchaykina *et al.*, 2025). To improve and modify BC yield and structure, the insitu fabrication was performed by mixing 50 ml of MHS medium with 50 ml of

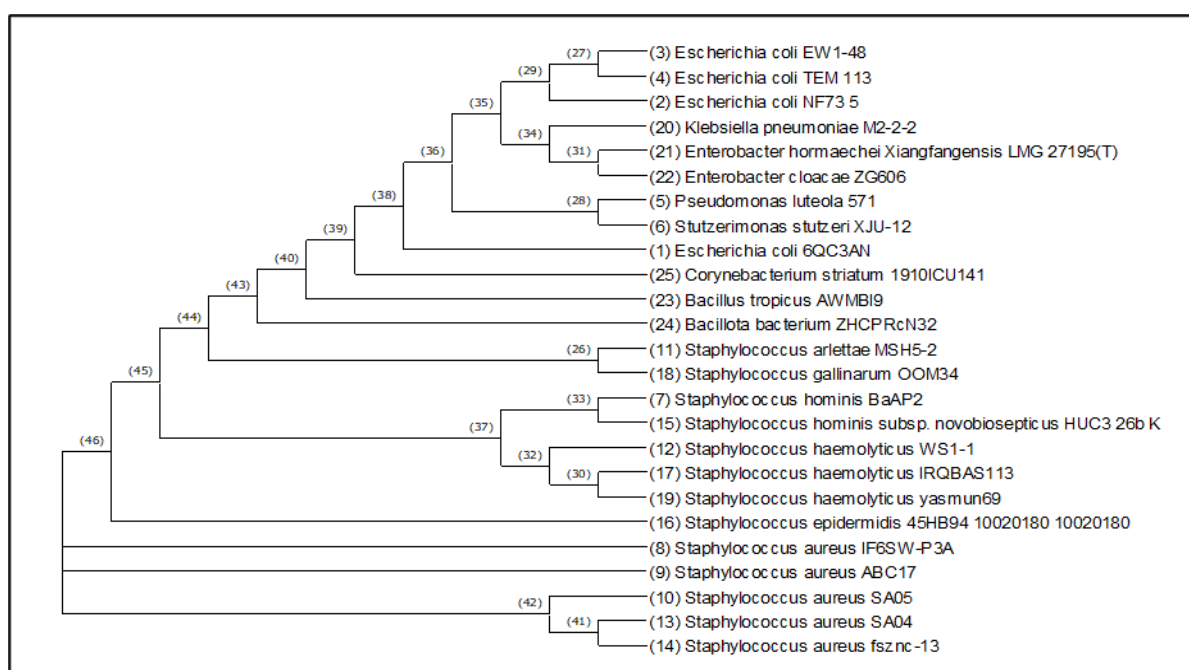


**Fig. 3.** Neighbor-Joining phylogenetic tree of 16S rRNA sequences showing relationships between bacterial isolates and GenBank reference strains (MEGA11, 1000 bootstrap replicates).

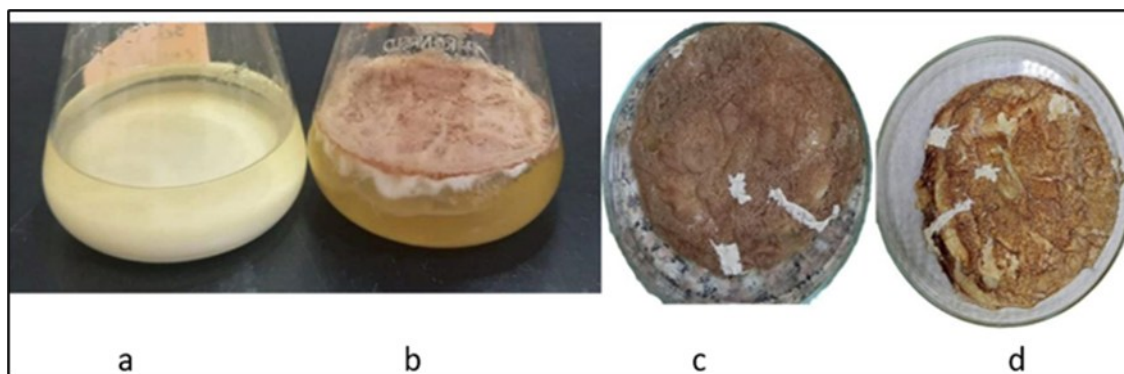


**Fig. 4.** Production of BC by isolates of *Bacillus licheniformis*: **a.** Control **b.** Medium with *Bacillus licheniformis* **c.** film before drying **d.** film after drying.

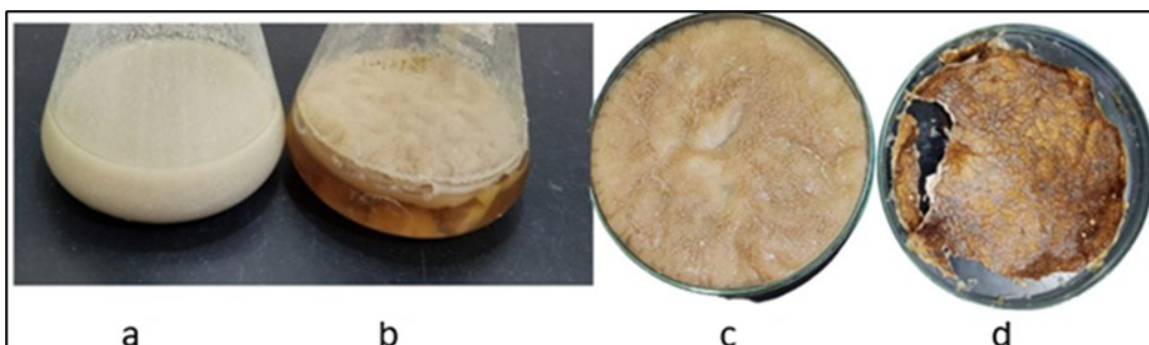


**Fig. 5.** In Situ fabrication of BC/GW produce by *B. licheniformis*: **a.** Control. **b.** Medium with *B. licheniformis*. **c.** film before drying. **d.** film after drying.

whey, 0.04%  $\text{FeCl}_3$ , and 0.025% gellan gum. Remarkably, the modified medium demonstrated a clear enhancement of BC/GW production (Fig. 5). The appearance of cellulose pellicles formed at the air-liquid interface after only 1-2 days of static conditions, suggests accelerated bacterial activity and growth, more notably, the resulting pellicles exhibited a thicker, more cohesive structure about 5 mm of thickness. The wet weight of BC/GW films increased significantly ( $p < 0.001$ ) to  $289.0 \pm 1.0$  g/l, while the dry weight was  $11.4 \pm 1.0$  g/l when compared to BC films.

This result is consistent with that of Wu *et al.* (2021) who utilize *Taonella mepensis* to synthesize bacterial cellulose (BC) from medicinal herb residues in China, where the addition of gellan gum significantly improved yields. The in situ fermentation technique is appealing for producing bacterial cellulose from inexpensive substrates, with the most widely used additions being agar, carboxymethyl cellulose, glycerol, ethanol, sodium alginate, and xanthan, all of which have a strong potential for BC production (Cheng *et al.*, 2017). Whey, a dairy by-product rich in lactose and proteins, is known to have a high biological value due to its protein content, amino acids, vitamins, lactic and citric acids, minerals like calcium, magnesium, and phosphorus, and other secondary bioactive compounds (Revin *et al.*, 2018). A study by Kolesovs *et al.* (2023) showed that suitable strains can effectively utilize whey to produce large

quantities of BC. Additionally, adding elements like  $\text{FeCl}_3$  to the culture medium enhanced bacterial growth, increasing BC yield, especially in bacteria isolated from environments rich in chemicals, such as oil reservoirs.

#### **Ex situ fabrication of BC/GW/SA/LEV**

The BC/GW/SA/LEV composite films, obtained after external processing and drying, exhibited highly desirable physical properties: thin layers with a soft, pleasant surface texture and maintained structural integrity during handling. They were flexible and foldable than the original BC and BC/GW films, which are typically stiff and brittle. Additionally, the films could be easily cut with basic tools, such as scissors or scalpels, reflecting their excellent workability and mechanical adaptability (Fig. 6). This result is consistent with previous studies (Saleh *et al.*, 2022; Agustin *et al.*, 2024). Ultrasonic treatment can reorganize BC nanofibers and reduce their crystallinity, resulting in softer, more flexible films. High-energy ultrasound has been shown to alter the fiber dimensions and nanostructure of BC, thereby promoting a more flexible network (Ybañez and Camacho, 2021). Furthermore, it has been reported that forming composites with polymers like alginate, gelatin, and glycerol significantly improves the softness and elasticity of BC (Chiaoprakobkij *et al.*, 2020). Glycerol can stretch polymer chains and break hydrogen bonds, increasing the material's elasticity and decreasing its ten-

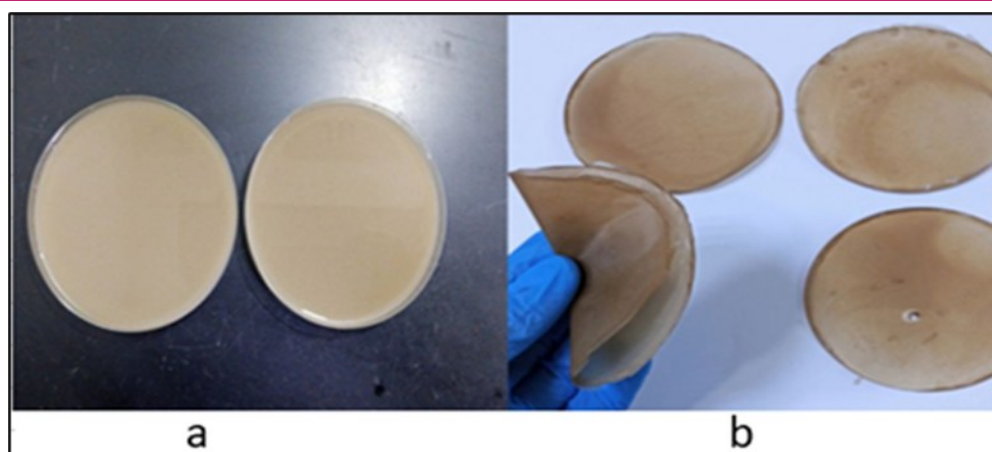


**Fig. 6.** Ex situ fabrication of BC/GW/SA/LEV films: a. Before drying. b. After drying

sile strength. The glycerol molecules enter the polymer matrix and fill the spaces between molecules via hydrogen bonds. This likely changes the polymer's structure, transforming it into a more disordered, flexible form with greater mobility (Agustin *et al.*, 2024).

#### Water holding capacity (WHC)

The WHC of spongy BC films was determined by measuring the difference between the wet and dry weights of the films before and after in situ fabrication. The results demonstrated that the modified medium not only affected BC yield but also its water-retention capacity. The BC/GW exhibited the highest WHC improvement at  $96.0 \pm 0.1$  % compared to non-fabricated BC films at  $93.94 \pm 0.59$  % ( $p=0.033$ ). This increase in water retention suggests possible structural modifications within the BC matrix that could enhance its water-absorption capacity. These findings agreed with Al-Hagar and Abol-Fotouh (2022).

#### Fourier transform infrared spectroscopy (FTIR)

FTIR spectroscopy was used to assess the molecular bonding and functional groups of BC, BC/GW, BC/GW/SA, and BC/GW/SA/LEV films (Fig. 7). For BC (Curve a), the native BC film's infrared spectrum revealed absorption peaks characteristic of this particular polymer. The peak of absorption in the one can be identified at  $3287.8 \text{ cm}^{-1}$ , corresponding to the stretching vibrations of hydroxyl groups in cellulose engaged in hydrogen-bond formation. The broader peak for BC indicated stronger OH bonding (Chen *et al.*, 2024). The intense band at 2925 and  $2865 \text{ cm}^{-1}$  corresponds to the stretching vibrations group of  $\text{CH}_2$  and CH groups. The band at  $1632.24 \text{ cm}^{-1}$  has been attributed to the  $\text{-COOH}$  group, which corresponds to the glucose carbonyl (Saleh *et al.*, 2020). Peaks at  $1026.3 \text{ cm}^{-1}$  were formed by the C-O-C group and hydroxyl C-O-H functional groups of the carbohydrate ring, consistent with earlier research (Qiu *et al.*, 2016). Furthermore, maxima for the C=O bending vibrations were found at 1596

$\text{cm}^{-1}$  and  $1539 \text{ cm}^{-1}$  (Almihiyawi *et al.*, 2024). In contrast to BC/GW (curve b), only two new peaks were observed at  $1740.4 \text{ cm}^{-1}$  and  $1096.57 \text{ cm}^{-1}$ . The stretch has been attributed to C-O, indicating that the fabrication of the medium exerted an influence, as new functional groups were observed. Furthermore, the band between  $1644.88 \text{ cm}^{-1}$  and  $1096.57 \text{ cm}^{-1}$  showed high intensities. In the case of BC/GW/SA (curve c), the interaction between SA and BC could be identified by the carboxyl and carbonyl group bands present in the range of  $1900\text{-}1500 \text{ cm}^{-1}$  (Saleh *et al.*, 2022). The band at  $1600.68$  showed high intensity, with two broad peaks at  $1594.6 \text{ cm}^{-1}$  and  $1547 \text{ cm}^{-1}$ . The peak at  $3286.7 \text{ cm}^{-1}$  showed higher intensity than that in BC/GW. This implies that there are more molecular bonds between BC, glycerol, and SA. The biocomposite, made from BC and chitosan with glycerol addition of 0.25-0.75%, demonstrated a similar outcome (Paluch *et al.*, 2022). The composite of BC/GW/SA/LEV (curve d) showed that many bands were shifted; for instance, in BC/GW/SA, the peak at  $1600.6 \text{ cm}^{-1}$  was just a shoulder, while the peak at  $1594.29 \text{ cm}^{-1}$  was easily observed in the composite loaded with the antibiotic. Two peaks centered at  $1401.13 \text{ cm}^{-1}$  and  $868 \text{ cm}^{-1}$  were shifted to  $1405.22 \text{ cm}^{-1}$  and  $862.71 \text{ cm}^{-1}$ , and the intensity of the peaks became stronger. This indicates a clear interaction between the composite, amine, and carboxylate groups of LEV. These results agreed with the study by Fatahi *et al.* (2021), who showed as levofloxacin was added to nanofibrous matrices, additional absorption peaks appeared in the  $400\text{-}1000 \text{ cm}^{-1}$  range ( $762.82$ ,  $602.77$ , and  $568.18 \text{ cm}^{-1}$ ), suggesting drug-matrix interactions. The peaks found indicated that the LEV molecules were successfully loaded into the BC/GW/SA/LEV composite.

#### BC films morphological characteristics as determined by SEM

Morphological analysis using SEM revealed gradual structural improvements resulting from the application

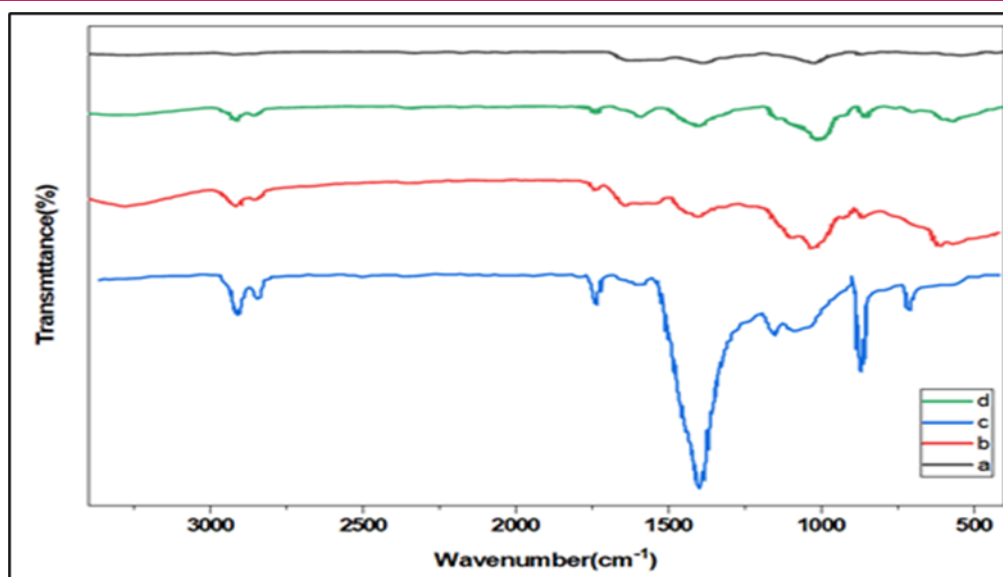


**Fig. 7.** FTIR analysis of the BC films: **a.** BC. **b.** BC/GW. **c.** BC/GW/SA. **d.** BC/GW/SA/LEV

of insitu and ex situ fabrication strategies to BC. Pure BC exhibited a homogeneous three-dimensional network of randomly interconnected microfibers, characterized by an irregular, rough surface reflecting the fibrous nature of cellulose. The fibres were relatively thick and large, with well-developed pores between them, forming a distinct porous structure (Fig. 8a, b). This morphology is consistent with the known properties of BC produced on glucose media (Fuller *et al.*, 2018; Bagewadi *et al.*, 2020; Mohammad *et al.*, 2023). The large surface area and numerous bonding sites in this porous structure provide an ideal platform for subsequent fabrication and loading. Insitu fabrication by adding gellan gum, whey, and FeCl<sub>3</sub> to the production medium resulted in significant structural improvements. BC/GW analysis revealed a denser and more cohesive fibrous network compared to pure BC, exhibiting tighter inter-fiber bonding and a marked decrease in pore size and number of voids (Fig.8 c, d). This morphological improvement suggests that bacterial activity was enhanced by the addition of the supplements, resulting in denser fibres and greater BC synthesis. These results are consistent with those of Wang *et al.* (2021), who reported that gellan gum increased bacterial cellulose production by up to 59% and modified its crystalline properties. Furthermore, the structural interaction between the added supplements and the cellulose molecules improved inter-bonding and internal cohesion, enhancing the mechanical strength and functional performance of the material (Rukmanikrishnan *et al.*, 2020).

*Ex situ* fabrication with the addition of SA significantly altered the composite's surface properties (Fig. 8e, f). Examination of BC/GW/SA revealed an interwoven network structure with a more homogeneous surface, in which a clear alginate gel layer surrounded the cellu-

lose fibres. This interweaving reflects the strength of hydrogen bonds between the hydrophilic alginate and cellulose molecules, resulting in improved interfacial adhesion and reduced pore size and number. The high density and low porosity indicate the success of the external fabrication process in enhancing the stability of the composite and filling the visible voids in BC/GW. The interwoven fibre structure within the alginate matrix suggests the potential to create an ideal polymer for drug diffusion and retention (Shahriari-Khalaji *et al.*, 2020; Saleh *et al.*, 2022; Munhoz *et al.*, 2024). *Ex situ* fabrication with Levofloxacin loading revealed characteristic morphological changes confirming successful drug incorporation. BC/GW/SA/LEV analysis revealed a branched, fibrous surface bearing shiny, radially oriented crystalline aggregates distributed heterogeneously among the fibres, representing the deposition and arrangement of levofloxacin molecules within the polymer matrix. These crystalline aggregates resulted in a marked increase in surface roughness, with density variations between regions, consistent with the molecular distribution of the drug across the polymer chains (Fig. 8 g, h). These observations are consistent with previous studies demonstrating similar morphological changes when drugs are loaded onto BC surfaces (Shao *et al.*, 2016; Saleh *et al.*, 2022; Kapourani *et al.*, 2024).

#### Thermogravimetric analysis (TGA)

Thermal analysis was performed on three films BC, BC/GW, and BC/GW/SA (Fig. 9). The results revealed a gradual improvement in thermal stability with each stage of fabrication. The BC film exhibited predicted thermal behavior consistent with the scientific literature. An initial weight loss of 13.5% was recorded between 0 –200°C, primarily attributed to the evaporation of mois-

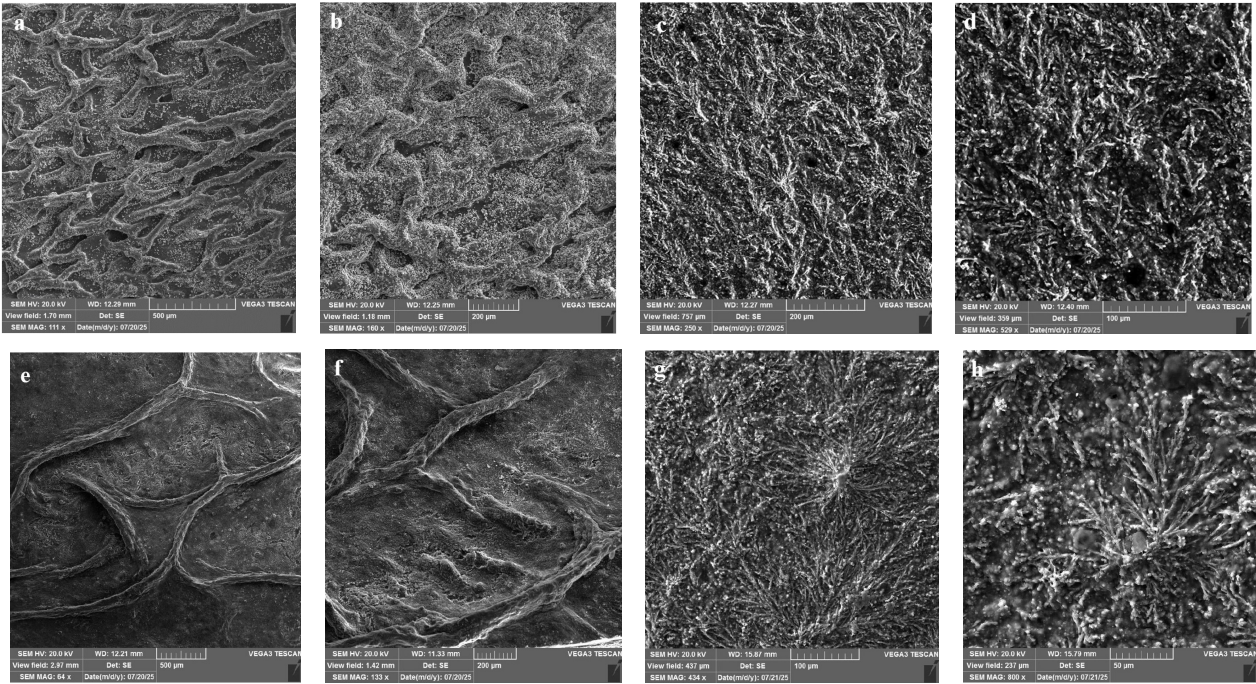


**Fig. 8.** Scanning electron microscopy images showing the films that were prepared. (a–b) Pure BC at magnifications of 111× and 160× reveals a dense fibrillar network formed by a randomly dispersed nanofibrous structure. The BC/GW composite at 250× and 529× magnifications shows a denser and more compact fibrous network with smaller pores (c–d) as a result of GW integration. (e–f) BC/GW/SA film with a more compact and uniform shape and enhanced structural integrity at 64× and 133× magnifications. (g–h) The BC/GW/SA/LEV film at 434× and 800× magnifications shows improved surface roughness and drug-loaded areas, demonstrating the effective integration of LEV

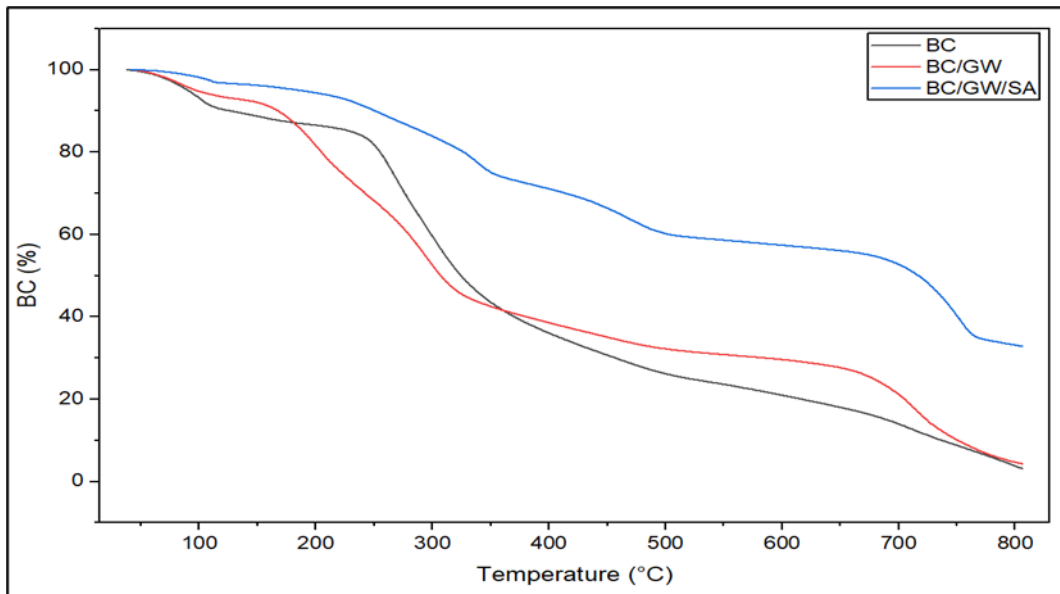


**Fig. 9.** Thermogravimetric analysis (TGA) curves of bacterial cellulose (BC) and its composites (BC/GW and BC/GW/SA) demonstrate weight loss behavior and thermal stability

ture trapped within the fibrous matrix (Sheykhnazari *et al.*, 2018; Kim and kim., 2024). Major degradation occurred between 200–400°C, with 64% weight loss, indicating the dissociation of cellulose chains and rupture of glycosidic bonds (Dhar *et al.*, 2019; Flores-Hernández *et al.*, 2021). Total weight loss reached 74% at 500°C, and a 50% loss was recorded at 324°C. At

806°C, only 3.1% of the original mass remained, confirming the near-complete thermal degradation of the material. The addition of gellan gum and whey resulted in changes in the thermal properties. The moisture content increased to 19% in the 0–200°C range, attributed to the hydrophilic nature of gellan gum and its high moisture retention capacity (Abdl Aali and Al-Sahlany,

**Table 3.** Antibacterial activity of BC/GW/SA/LEV on pathogenic bacterial isolates

Bacterial strains	Concentrations of levofloxacin/Inhibition zone diameter(mm)					
	7.5mg	5.0mg	2.5mg	1.0mg	0.5mg	0.1mg
<i>Escherichia coli</i> strain R61	11.0±1.0	11.0±1.0	8.0±1.0	0.0±0.0	0.0±0.0	0.0±0.0
<i>Pseudomonas luteola</i> strain 571	32.0±1.0	31.0±1.0	31.0±1.0	28.0±1.0	23.0±1.0	22.0±1.0
<i>Staphylococcus hominis</i> strain BaAP2	33.0±1.0	30.0±1.0	29.0±1.0	28.0±1.0	28.0±1.0	25.0±1.0
<i>Staphylococcus aureus</i> Strain IF6SW-P3A	33.0±1.0	32.0±1.0	30.0±1.0	20.0±1.0	19.0±1.0	17.0±1.0
<i>Staphylococcus aureus</i> strain ABC17	32.0±1.0	31.0±1.0	30.0±1.0	25.0±1.0	20.0±1.0	18.0±1.0
<i>Escherichia coli</i> strain EW1-48	12.0±1.0	12.0±1.0	8.0±1.0	0.0±0.0	0.0±0.0	0.0±0.0
<i>Staphylococcus aureus</i> strain SA05	20.0±1.0	15.0±1.0	8.0±1.0	0.0±0.0	0.0±0.0	0.0±0.0
<i>Bacillus tropicus</i> strain AWMBI9	31.0±1.0	30.0±1.0	29.0±1.0	22.0±1.0	20.0±1.0	19.0±1.0
<i>Pseudomonas iranica</i> strain GH10	33.0±1.0	33.0±1.0	32.0±1.0	32.0±1.0	32.0±1.0	30.0±1.0
<i>Escherichia coli</i> strain TEM 113	20.0±1.0	15.0±1.0	10.0±1.0	0.0±0.0	0.0±0.0	0.0±0.0
<i>Staphylococcus haemolyticus</i> strain yas-mun69	12.0±1.0	12.0±1.0	0.0±0.0	0.0±0.0	0.0±0.0	0.0±0.0
<i>Klebsiella pneumoniae</i> strain M2-2-2	31.0±1.0	30.0±1.0	30.0±1.0	26.0±1.0	24.0±1.0	21.0±1.0
<i>Enterobacter cloacae</i> strain ZG606	33.0±1.0	32.0±1.0	30.0±1.0	29.0±1.0	24.0±1.0	21.0±1.0
<i>Bacillota bacterium</i> strain ZHCPRcN32	35.0±1.0	31.0±1.0	30.0±1.0	24.0±1.0	18.0±1.0	17.0±1.0
<i>Staphylococcus haemolyticus</i> strain WS1-1	32.0±1.0	32.0±1.0	30.0±1.0	30.0±1.0	29.0±1.0	28.0±1.0
<i>Staphylococcus gallinarum</i> strain OOM34	31.0±1.0	29.0±1.0	28.0±1.0	18.0±1.0	17.0±1.0	13.0±1.0
<i>Staphylococcus haemolyticus</i> IRQBAS113	23.0±1.0	19.0±1.0	14.0±1.0	13.0±1.0	0.0±0.0	0.0±0.0

\*Mean ± SD, n=3, P ≤ 0.001

2024). Despite this increase, the thermal decomposition pattern remained similar to that of pure BC, with a 62% loss recorded between 200–400°C and 68% at 500°C. The temperature at which 50% of the mass was lost decreased slightly to 306°C. The remaining mass at 805°C was 4.3%, which is almost identical to that of BC. These results confirm that internal fabrication did not negatively affect the basic structure of BC (Wu *et al.*, 2021). The BC/GW/SA composite exhibited exceptionally improved thermal stability compared to previous films. Initial weight loss decreased significantly to only 6% at 0–200°C, reflecting a substantial improvement in moisture retention. This improvement is attributed to the formation of a denser polymer network via hydrogen bonds between the hydroxyl groups in BC and the carboxyl groups in SA, thus limiting water evaporation (Agustin *et al.*, 2021; Wai Chun *et al.*, 2021). Importantly, the degradation rate decreased significantly to only 29% in the 200–400°C range, com-

pared to 64% and 62% for previous films. This marked improvement is explained by the unique properties of SA, which exhibits three degradation phases at 103°C, 212°C, and 426°C (Flores-Hernandez *et al.*, 2021). The temperature at which 50% of the weight was lost rose to an exceptional 716°C, highlighting the compound's superior thermal resistance (Agha and Kati, 2025). Furthermore, the remaining mass at 805°C reached 32.8%, a remarkable increase attributed to the formation of thermally stable inorganic structures such as Na<sub>2</sub>CO<sub>3</sub> from the decomposition of SA. This marked improvement in the thermal stability and structural integrity of the BC/GW/SA membrane makes it an ideal candidate for drug delivery applications.

#### Antibacterial activity of BC/GW/SA/LEV

The antibacterial efficacy of a BC/GW/SA/LEV composite at varying concentrations of levofloxacin was assessed by the disk diffusion technique. The BC and

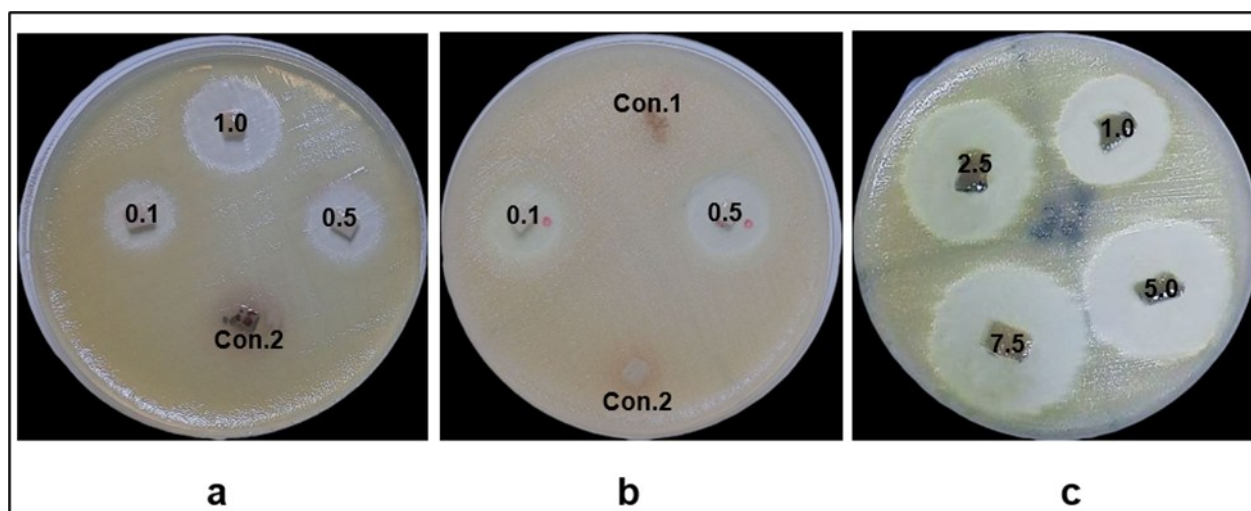


**Fig. 10.** Effect of BC/GW/SA/LEV on pathogenic bacteria: **a.** F09. **b.** B12. **c.** B09

BC/GW/SA composites showed no activity against pathogenic bacteria, as indicated in (Table 3) and (Fig. 10). This result agrees with a previous investigation (Saleh *et al.*, 2022). BC is inherently biologically inert and lacks intrinsic antimicrobial properties, as demonstrated in previous studies (Lahiri *et al.*, 2021; Swingler *et al.*, 2021). Similarly, gellan gum is primarily used as a structural and carrier material without intrinsic antimicrobial properties (Guo *et al.*, 2020). Other studies have also confirmed that SA is not inherently antimicrobial and requires chemical combination with antibiotics (Lee *et al.*, 2023; Kalkan *et al.*, 2025). Therefore, the lack of antibacterial activity in the base compounds (BC, BC/GW/SA) is consistent with the known properties of these components, and confirms that the observed antimicrobial activity is entirely attributable to the presence of levofloxacin in the composite of BC/GW/SA/LEV. The results demonstrate the successful incorporation of levofloxacin into the BC/GW/SA composite matrix. According to these findings, the antibacterial efficacy of BC/GW/SA/LEV composites against pathogenic bacteria increased with increasing LEV concentration. The maximum inhibition zone of *Bacillota bacterium* strain ZHCPRcN32 was 35 mm at a concentration of 7.5 mg, while the lowest was against *Escherichia coli* at 11 mm in the same concentration. Many strains showed high susceptibility to antibiotics at different concentrations; antimicrobial activity may be due to varying susceptibilities of the microbes to the prepared composites. Levofloxacin belongs to the quinolone family, a class of bactericidal antibiotics that directly kill bacterial cells by inhibiting the vital enzymes topoisomerase II (DNA gyrase) and topoisomerase IV. This results in the conversion of these enzymes into toxic agents that cause permanent breaks in bacterial chromosomes, leading to cell death (Yefet *et al.*, 2018). This finding is agreed with previous study (Gromovych *et al.*, 2017). A number of investigations documented

that BC films were made using additional materials to improve their action, such as BC/SA/GM (Saleh *et al.*, 2022), BC/SA/silver nanoparticles (Yang *et al.*, 2017), and BC/SA/chitosan/copper sulfate (Wichai *et al.*, 2019). The antibacterial efficacy of the compound was assessed using an in vitro disc diffusion assay, but this does not replicate the complexities of in vivo conditions, such as immune responses, fluid flow, sustained drug release, or biofilm penetration. Therefore, despite the encouraging in vitro results, in vivo studies are needed to confirm its therapeutic efficacy.

## Conclusion

*Staphylococcus* sp. was the most frequently recovered genus from a variety of wound and burn infections. *Bacillus licheniformis* was quite effective in BC production. With unique qualities that set it apart from other forms of cellulose, in situ and ex situ production enhances the functional properties and yields of BC. The incorporation of antibiotics into BC composites for the treatment of pathogenic bacteria provided efficient antibacterial activity and can serve as a promising platform for localized support of antibiotic delivery. To improve long-term antibacterial activity and reduce the likelihood of resistance development, more adjustments of antibiotic loading and release patterns are advised.

## Conflict of interest

The authors declare that they have no conflict of interest.

## REFERENCES

1. Abdl Aali, R. A. K. & Al-Sahlany, S. T. G. (2024). Gellan gum as a unique microbial polysaccharide: Its characteristics, synthesis, and current application trends. *Gels*, 10 (3), 183. <https://doi.org/10.3390/gels10030183>
2. Aboud, E. M., Burghal, A. & Laftah, A. H. (2021). Genetic

- identification of hydrocarbons degrading bacteria isolated from oily sludge? and petroleum-contaminated soil in Basrah City, Iraq. *Biodiversitas Journal of Biological Diversity*, 22(4). 10.13057/diodiv/d220441 <https://doi.org/10.13057/biodiv/d220441>
3. Agha, T. & Kati, A. (2025). Development of functional bacterial cellulose composites from Kombucha waste for biodegradable food packaging. *Discover Applied Sciences*, 7(8), 840. <https://doi.org/10.1007/s42452-025-07145-4>
  4. Agustin, S., Cahyanto, M. N. & Wahyuni, E. T. (2024, July). Effect of glycerol plasticizer on the structure and characteristics of bacterial cellulose-based biocomposite films. In *IOP Conference Series: Earth and Environmental Science*, (1377, 1, p. 012046). IOP Publishing. [https://doi.org/10.1088/1755-1315/1377/1/012046?urlappend=%3Futm\\_source%3Dresearchgate.net%26utm\\_medium%3Darticle](https://doi.org/10.1088/1755-1315/1377/1/012046?urlappend=%3Futm_source%3Dresearchgate.net%26utm_medium%3Darticle)
  5. Agustin, S., Wahyuni, E. T., Suparmo, S., Supriyadi, S. & Cahyanto, M. N. (2021). Production and characterization of bacterial cellulose-alginate biocomposites as food packaging material. *Food Research*, 5(6), 204-210. [https://doi.org/10.26656/fr.2017.5\(6\).733](https://doi.org/10.26656/fr.2017.5(6).733)
  6. AL-assdy, H. Q., Al-Tamimi, W.H. & Almansoori, A.F. (2025). Molecular detection of bacteria isolated from polluted environments and screening their ability to produce extracellular biopolymer flocculants. *Beni-Suef University Journal of Basic and Applied Sciences*, 14(1), 29-41. <https://doi.org/10.1186/s43088-025-00621-1>
  7. Al-Hagar, O. E. & Abol-Fotouh, D. (2022). A turning point in the bacterial nanocellulose production employing low doses of gamma radiation. *Scientific Reports*, 12(1), 7012. <https://doi.org/10.1038/s41598>
  8. AlHawaj, A., AlMadhoob, M., Alkhanaizi, R. & AlHaddad, A. (2024). Evaluation of white blood cell count, lymphocyte percentage, neutrophil percentage, and elevated temperature as predictors of wound infection in burn patients. *Cureus*, 16(6). <https://doi.org/10.13057/biodiv/d240519>
  9. Almihiyawi, R. A. H., Musazade, E., Alhussany, N., Zhang, S. & Chen, H. (2024). Production and characterization of bacterial cellulose by *Rhizobium* sp. isolated from bean root. *Scientific Reports*, 14(1), 10848. <https://doi.org/10.1038/s41598-024-61619-w>
  10. Alsarhan, I. & Çam, S. (2023). Antibiotic resistance of *Escherichia coli* isolates obtained from burn patients. *Gümüşhane Üniversitesi Fen Bilimleri Dergisi*, 13(4), 780-789. <https://doi.org/10.17714/gumusfenbil.1271503>
  11. Al-Shami, H. G. A., Al-Tamimi, W. H. & Hateet, R. R. (2023). The antioxidant potential of copper oxide nanoparticles synthesized from a new bacterial strain. *Biodiversitas Journal of Biological Diversity*, 24(5). <https://doi.org/10.13057/biodiv/d240519>
  12. Alyousif, N. A., Al-Tamimi, W. H. & Abd Al-sahib, M. A. (2022). Evaluation of the effect of various nutritional and environmental factors on biosurfactant production by *Staphylococcus epidermidis*. *Biodiversitas Journal of Biological Diversity*, 23(7). <https://doi.org/10.13057/biodiv/d230729>
  13. Al-zaidi, M. H. H., Al-Tamimi, W. H. & Saleh, A. A. A. (2023). Molecular determination of the microbial diversity associated with vaginitis and testing their sensitivity to selected antimicrobials. *Biodiversitas Journal of Biological Diversity*, 24(8). <https://doi.org/10.13057/biodiv/d240806>
  14. Aswini, K., Gopal, N. O. & Uthandi, S. (2020). Optimized culture conditions for bacterial cellulose production by *Acetobacter senegalensis* MA1. *BMC Biotechnology*, 20(1), 46. <https://doi.org/10.1186/s12896-020-00639-6>
  15. Atta, O. M., Manan, S., Ul-Islam, M., Ahmed, A. A. Q., Ullah, M. W. & Yang, G. (2021). Silver decorated bacterial cellulose nanocomposites as antimicrobial food packaging materials. *ES Food & Agroforestry*, 6(26), 12-26. <http://dx.doi.org/10.30919/esfaf590>
  16. Avcioglu N. H. (2022). Bacterial cellulose: recent progress in production and industrial applications. *World Journal of Microbiology & Biotechnology*, 38(5), 86. <https://doi.org/10.1007/s11274-022-03271-y>
  17. Aydin, Y. A. & Aksoy, N. D. (2014). Isolation and characterization of an efficient bacterial cellulose producer strain in agitated culture: *Gluconacetobacter hansenii* P2A. *Applied Microbiology And Biotechnology*, 98(3), 1065-1075. <https://doi.org/10.1007/s00253-013-5296-9>
  18. Bagewadi, Z. K., Bhavikatti, J. S., Muddapur, U. M., Yaranguppi, D. A. & Mulla, S. I. (2020). Statistical optimization and characterization of bacterial cellulose produced by isolated thermophilic *Bacillus licheniformis* strain ZBT2. *Carbohydrate Research*, 491, 107979. <https://doi.org/10.1016/j.carres.2020.107979>
  19. Barry, M. (2021). *Pseudomonas luteola* bacteremia in newly diagnosed systemic lupus erythematosus. *Case Reports in Infectious Diseases*, 2021(1), 4051378. <https://doi.org/10.1155/2021/4051378>
  20. Bekatorou, A., Plioni, I., Sparou, K., Maroutsidou, R., Tsafraikidou, P., Petsi, T. & Kordouli, E. (2019). Bacterial cellulose production using the corinthian currant finishing side-stream and cheese whey: process optimization and textural characterization. *Foods*, 8(6), 193. <https://doi.org/10.3390/foods8060193>
  21. Bhujugade, S. R., Karande, G. & Patil, S. (2024). Bacteriological profile and antibiogram pattern of wound infection in a tertiary care hospital. *Cureus*, 16(10), e72185. <https://doi.org/10.7759/cureus.72185>
  22. Cazón, P. & Vázquez, M. (2021). Improving bacterial cellulose films by ex-situ and in-situ modifications: A review. *Food Hydrocolloids*, 113, 106514. <https://doi.org/10.1016/j.foodhyd.2020.106514>
  23. Chamoun, M. N. & Gonzalez Matheus, G. (2025). Complement in chronic wound infections: complementary or a cascade of chaos?. *Microbiology Australia*, 46(2), 58-62. <https://doi.org/10.1071/MA25019>
  24. Chaudhary, N. A., Munawar, M. D., Khan, M. T., Rehan, K., Sadiq, A., Tameez-Ud-Din, A., Bhatti, H. W. & Rizvi, Z. A. (2019). Epidemiology, bacteriological profile, and antibiotic sensitivity pattern of burn wounds in the burn unit of a tertiary care hospital. *Cureus*, 11(6), e4794. <https://doi.org/10.7759/cureus.4794>
  25. Chen, J., Hong, F., Zheng, H., Zheng, L. & Du, B. (2024). Using static culture method to increase the production of *Acetobacter xylinum* bacterial cellulose. *Journal of Natural Fibers*, 21(1), 2288286. <https://doi.org/10.1080/15440478.2023.2288286>
  26. Cheng, Z., Yang, R., Liu, X., Liu, X. & Chen, H. (2017). Green synthesis of bacterial cellulose via acetic acid pre-

- hydrolysis liquor of agricultural corn stalk used as carbon source. *Bioresource Technology*, 234, 8-14. <https://doi.org/10.1016/j.biortech.2017.02.131>
27. Chiaoprakobkij, N., Suwanmajo, T., Sanchavanakit, N. & Phisalaphong, M. (2020). Curcumin-loaded bacterial cellulose/alginate/gelatin as a multifunctional biopolymer composite film. *Molecules*, 25(17), 3800. <https://doi.org/10.3390/molecules25173800>
  28. Devi, A. R., Vijayalakshmi, J., Kumari, S. S. & Kumar, A. P. (2024). A study on time related changes in bacterial pattern in burn wound infections and their antibiogram in a tertiary care hospital. *International Journal of Pharmaceutical and Clinical Research*, 16(1), 1591–1596. <https://doi.org/10.5281/zenodo.11128996>
  29. Dhar, P., Etula, J. & Bankar, S. B. (2019). In situ bioprocessing of bacterial cellulose with graphene: percolation network formation, kinetic analysis with physicochemical and structural properties assessment. *ACS Applied Bio Materials*, 2(9), 4052-4066. <https://doi.org/10.1021/acssabm.9b00581>
  30. Dissemond, J., Rembe, J. D., Assenheimer, B., Barysch Bonderer, M., Gerber, V., Kottner, J., ... & Schwarzkopf, A. (2025). Systematics, diagnosis and treatment of wound infections in chronic wounds: A position paper from WundDACH. *JDDG: Journal der Deutschen Dermatologischen Gesellschaft*, 23(5), 565-574. <https://doi.org/10.1111/ddg.15649>
  31. Fatahi, Y., Sanjabi, M., Rakhshani, A., Motasadizadeh, H., Darbasizadeh, B., Bahadorikhaili, S. & Farhadnejad, H. (2021). Levofloxacin-halloysite nanohybrid-loaded fibers based on poly (ethylene oxide) and sodium alginate: Fabrication, characterization, and antibacterial property. *Journal of Drug Delivery Science and Technology*, 64, 102598. <https://doi.org/10.1016/j.jddst.2021.102598>
  32. Flores-Hernández, C. G., Cornejo-Villegas, M. D. L. A., Moreno-Martell, A. & Del Real, A. (2021). Synthesis of a biodegradable polymer of poly (sodium alginate/ethyl acrylate). *Polymers*, 13(4), 504. <https://doi.org/10.3390/polym13040504>
  33. Fuller, M. E., Andaya, C. & McClay, K. (2018). Evaluation of ATR-FTIR for analysis of bacterial cellulose impurities. *Journal of Microbiological Methods*, 144, 145-151. <https://doi.org/10.1016/j.mimet.2017.10.017>
  34. Gromovych, T. I., Sadykova, V. S., Lutchenko, S. V., Dmitrenok, A. S., Feldman, N. B., Danilchuk, T. N. & Kashirin, V. V. (2017). Bacterial cellulose synthesized by *Gluconacetobacter hansenii* for medical applications. *Applied Biochemistry and Microbiology*, 53(1), 60-67. <https://link.springer.com/article/10.1134/s0003683817010094>
  35. Guo, N., Zhu, G., Chen, D., Wang, D., Zhang, F. & Zhang, Z. (2020). Preparation and characterization of gellan gum–guar gum blend films incorporated with nisin. *Journal of Food Science*, 85(6), 1799-1804. <https://doi.org/10.1111/1750-3841.15143>
  36. Hamel, A. H., Al-Tamimi, W. H. & Fayadh, M. H. (2026). Bacterial diversity in oil field environments and evaluation of their ability to biosynthesize silver nanoparticles (AgNPs). *Nature Environment and Pollution Technology*, 25(1), D1801. <https://doi.org/10.46488/NEPT.2026.v25i01.D1801>
  37. Hamzah, A. F., Al-Mossawy, M. I., Al-Tamimi, W. H., Al-Najm, F. M. & Hameed, Z. M. (2020). Enhancing the spontaneous imbibition process using biosurfactants produced from bacteria isolated from Al-Rafidiya oil field for improved oil recovery. *Journal of Petroleum Exploration and Production Technology*, 10(8), 3767-3777. <https://doi.org/10.1007/s13202-020-00874-9>
  38. Kalkan, S., Çopur, Ş. Y., Akben, S. B., Otağ, M. R. & Engin, M. S. (2025). Effect of incorporation of mix probiotic culture in sodium alginate film characteristics: antimicrobial, physicochemical, mechanical, and barrier properties. *Probiotics And Antimicrobial Proteins*, 17(5), 3774–3789. <https://doi.org/10.1007/s12602-025-10651-x>
  39. Kapourani, A., Katopodis, K., Valkanioti, V., Chatzithodoridou, M., Cholevas, C. & Bampalexis, P. (2024). Evaluation of suitable polymeric matrix/carriers during loading of poorly water soluble drugs onto mesoporous silica: Physical stability and in vitro supersaturation. *Polymers*, 16(6), 802. <https://doi.org/10.3390/polym16060802>
  40. Khalid, F., Poulouse, C., Farah, D. F. M., Mahmood, A., Elsheikh, A. & Khojah, O. T. (2024). Prevalence and antimicrobial susceptibility patterns of wound and pus bacterial pathogens at a tertiary care hospital in Central Riyadh, Saudi Arabia. *Microbiology Research*, 15(4), 2015-2034. <https://doi.org/10.3390/microbiolres15040135>
  41. Kim, H. & Kim, H. R. (2024). Improved flame retardancy and mechanical properties of bacterial cellulose fabrics via solvent exchange and entrapment of zein and gluten. *Fashion and Textiles*, 11(1), 28. <https://doi.org/10.1186/s40691-024-00395-7>
  42. Kolesovs, S., Ruklisha, M. & Semjonovs, P. (2023). Synthesis of bacterial cellulose by *Komagataeibacter rhaeticus* MSCL 1463 on whey. *3 Biotech*, 13(3), 105. <https://doi.org/10.1007/s13205-023-03528-9>
  43. Lahiri, D., Nag, M., Dutta, B., Dey, A., Sarkar, T., Pati, S., ... & Ray, R. R. (2021). Bacterial cellulose: Production, characterization, and application as antimicrobial agent. *International Journal Of Molecular Sciences*, 22(23), 12984. <https://doi.org/10.3390/ijms222312984>
  44. Lee, M., Rüegg, N. & Yildirim, S. (2023). Evaluation of the antimicrobial activity of sodium alginate films integrated with cinnamon essential oil and citric acid on sliced cooked ham. *Packaging Technology and Science*, 36(8), 647-656. <https://doi.org/10.1002/pts.2733>
  45. Machado, R. T., Gutierrez, J., Tercjak, A., Trovatti, E., Uahib, F. G., de Padua Moreno, G., ... & Barud, H. S. (2016). *Komagataeibacter rhaeticus* as an alternative bacteria for cellulose production. *Carbohydrate Polymers*, 152, 841-849. <https://doi.org/10.1016/j.carbpol.2016.06.049>
  46. Maitz, J., Merlino, J., Rizzo, S., McKew, G. & Maitz, P. (2023). Burn wound infections microbiome and novel approaches using therapeutic microorganisms in burn wound infection control. *Advanced Drug Delivery Reviews*, 196, 114769. <https://doi.org/10.1016/j.addr.2023.114769>
  47. Malcı, K., Li, I. S., Kisseroudis, N. & Ellis, T. (2024). Modulating microbial materials-engineering bacterial cellulose with synthetic biology. *ACS Synthetic Biology*, 13(12), 3857-3875. <https://doi.org/10.1021/acssynbio.4c00615>
  48. MMasoud, S. M., Ibrahim, R. A., Abd El-Baky, R. M. & Abd El-Rahman, S. A. (2020). Prevalence of bla<sub>CTX-M</sub> gene among MDR *Escherichia Coli* isolated from wound

- infections in minia university hospital, Egypt. *Minia Journal of Medical Research*, 31(4), 13-19. <https://doi.org/10.21608/mjmr.2022.214424>
49. Mohammad, N., El-Nour, A., Abd El-Ghafar, S., Roushdy, M. & Hammad, A. (2023). Bacterial cellulose loaded with amoxicillin/flucloxacillin: innovate tool for antibacterial applications. *Arab Journal of Nuclear Sciences and Applications*, 56(4), 91-100. <https://doi.org/10.21608/ajnsa.2023.183094.1700>
  50. Monk, E. J. M., Jones, T. P. W., Bongomin, F., Kibone, W., Nsubuga, Y., Ssewante, N., Muleya, I., Nsenga, L., Rao, V. B. & van Zandvoort, K. (2024). Antimicrobial resistance in bacterial wound, skin, soft tissue and surgical site infections in Central, Eastern, Southern and Western Africa: A systematic review and meta-analysis. *PLOS Global Public Health*, 4(4), e0003077. <https://doi.org/10.1371/journal.pgph.0003077>
  51. Mosaffa, F., Saffari, F., Veisi, M. & Tadjrobehkar, O. (2024). Some virulence genes are associated with antibiotic susceptibility in *Enterobacter cloacae* complex. *BMC Infectious Diseases*, 24(1), 711. <https://doi.org/10.1186/s12879>
  52. Munhoz, L. L. D. S., Guillens, L. C., Alves, B. C., Nascimento, M. G. O. F. D., Meneguim, A. B., Carbinatto, F. M., ... & Caetano, G. F. (2024). Bacterial nanocellulose/calcium alginate hydrogel for the treatment of burns. *Acta Cirúrgica Brasileira*, 39, e393324. <https://doi.org/10.1590/acb393324>
  53. Murray, C. J., Ikuta, K. S., Sharara, F., Swetschinski, L., Aguilar, G. R., Gray, A., ... & Tasak, N. (2022). Global burden of bacterial antimicrobial resistance in 2019: a systematic analysis. *The Lancet*, 399(10325), 629-655. [https://doi.org/10.1016/S0140-6736\(21\)02724-0](https://doi.org/10.1016/S0140-6736(21)02724-0)
  54. Ndikubwimana, I., Gahamanyi, N., Bwanakweli, T., Uwayo, H. D., Habimana, G. & Rogo, T. (2024). Case report: Pan-drug resistant *Pseudomonas aeruginosa* from a child with an infected burn wound at the university teaching hospital of Kigali, Rwanda. *Infection and Drug Resistance*, 4637-4642. <https://doi.org/10.2147/IDR.S486519>
  55. Orlando, I., Basnett, P., Nigmatullin, R., Wang, W., Knowles, J. C. & Roy, I. (2020). Chemical modification of bacterial cellulose for the development of an antibacterial wound dressing. *Frontiers in Bioengineering and Biotechnology*, 8, 557885. <https://doi.org/10.3389/fbioe.2020.557885>
  56. Paluch, M., Ostrowska, J., Tyński, P., Sadurski, W. & Konkol, M. (2022). Structural and thermal properties of starch plasticized with glycerol/urea mixture. *Journal of Polymers and the Environment*, 30(2), 728-740. <https://doi.org/10.1007/s10924-021-02235-x>
  57. Parchaykina, M. V., Liyaskina, E. V., Bogatyreva, A. O., Baykov, M. A., Gotina, D. S., Arzhanov, N. E., ... & Revin, V. V. (2025). Cost-effective production of bacterial cellulose and tubular materials by cultivating *Komagataeibacter sucrofermentans* B-11267 on a molasses medium. *Polymers*, 17(2), 179. <https://doi.org/10.3390/polym17020179>
  58. Phong, H. X., Lin, L. T., Thanh, N. N., Long, B. H. & Dung, N. T. (2017). Investigating the conditions for nata-de-coco production by newly isolated *Acetobacter* sp. *American Journal of Food Science and Nutrition*, 4(1), 1-6.
  59. Portela, R., Leal, C. R., Almeida, P. L. & Sobral, R. G. (2019). Bacterial cellulose: a versatile biopolymer for wound dressing applications. *Microbial Biotechnology*, 12(4), 586-610. <https://doi.org/10.1111/1751-7915.13392>
  60. Qiu, Y., Qiu, L., Cui, J. & Wei, Q. (2016). Bacterial cellulose and bacterial cellulose-vaccarin membranes for wound healing. *Materials Science and Engineering: C*, 59, 303-309. <https://doi.org/10.1016/j.msec.2015.10.016>
  61. Rahim Hateet R. (2021). Isolation and identification of some bacteria contemn in burn wounds in Misan, Iraq. *Archives of Razi Institute*, 76(6), 1665-1670. <https://doi.org/10.22092/ari.2021.356367.1833>
  62. Raiszadeh-Jahromi, Y., Rezazadeh-Bari, M., Almasi, H. & Amiri, S. (2020). Optimization of bacterial cellulose production by *Komagataeibacter xylinus* PTCC 1734 in a low-cost medium using optimal combined design. *Journal Of Food Science and Technology*, 57(7), 2524-2533. <https://doi.org/10.1007/s13197-020-04289-6>
  63. Revin, V., Liyaskina, E., Nazarkina, M., Bogatyreva, A. & Shchankin, M. (2018). Cost-effective production of bacterial cellulose using acidic food industry by-products. *Brazilian Journal of Microbiology* : [publication of the Brazilian Society for Microbiology], 49 Suppl 1(Suppl 1), 151-159. <https://doi.org/10.1016/j.bjm.2017.12.012>
  64. Rukmanikrishnan, B., Ramalingam, S., Rajasekharan, S. K., Lee, J. & Lee, J. (2020). Binary and ternary sustainable composites of gellan gum, hydroxyethyl cellulose and lignin for food packaging applications: Biocompatibility, antioxidant activity, UV and water barrier properties. *International Journal Of Biological Macromolecules*, 153, 55-62. <https://doi.org/10.1016/j.ijbiomac.2020.03.016>
  65. Saleh, A. K., El-Gendi, H., Soliman, N. A., El-Zawawy, W. K. & Abdel-Fattah, Y. R. (2022). Bioprocess development for bacterial cellulose biosynthesis by novel *Lactiplantibacillus plantarum* isolate along with characterization and antimicrobial assessment of fabricated membrane. *Scientific Reports*, 12(1), 2181. <https://doi.org/10.1038/s41598-022-06117-7>
  66. Saleh, A. K., Soliman, N. A., Farrag, A. A., Ibrahim, M. M., El-Shinnawy, N. A. & Abdel-Fattah, Y. R. (2020). Statistical optimization and characterization of a biocellulose produced by local Egyptian isolate *Komagataeibacter hansenii* AS. 5. *International Journal of Biological Macromolecules*, 144, 198-207. <https://doi.org/10.1016/j.ijbiomac.2019.12.103>
  67. Serrano-Aroca, Á., Cano-Vicent, A., i Serra, R. S., El-Tanani, M., Aljabali, A., Tambuwala, M. M. & Mishra, Y. K. (2022). Scaffolds in the microbial resistant era: Fabrication, materials, properties and tissue engineering applications. *Materials Today Bio*, 16, 100412. <https://doi.org/10.1016/j.mtbio.2022.100412>
  68. Shahriari-Khalaji, M., Hong, S., Hu, G., Ji, Y. & Hong, F. F. (2020). Bacterial nanocellulose-enhanced alginate double-network hydrogels cross-linked with six metal cations for antibacterial wound dressing. *Polymers*, 12(11), 2683. <https://doi.org/10.3390/polym12112683>
  69. Shao, W., Liu, H., Wang, S., Wu, J., Huang, M., Min, H. & Liu, X. (2016). Controlled release and antibacterial activity of tetracycline hydrochloride-loaded bacterial cellulose composite membranes. *Carbohydrate Polymers*, 145, 114-120. <https://doi.org/10.1016/>

- j.carbpol.2016.02.065
70. Sheykhnazari, S., Tabarsa, T., Mashkour, M., Khazaeian, A. & Ghanbari, A. (2018). Multilayer bacterial cellulose/resole nanocomposites: Relationship between structural and electro-thermo-mechanical properties. *International Journal of Biological Macromolecules*, 120, 2115-2122. <https://doi.org/10.1016/j.ijbiomac.2018.09.047>
  71. Stumpf, T. R., Yang, X., Zhang, J. & Cao, X. (2018). In situ and ex situ modifications of bacterial cellulose for applications in tissue engineering. *Materials Science and Engineering: C*, 82, 372-383. <https://doi.org/10.1016/j.msec.2016.11.121>
  72. Sulaeva, I., Hettegger, H., Bergen, A., Rohrer, C., Kostic, M., Konnerth, J., ... & Potthast, A. (2020). Fabrication of bacterial cellulose-based wound dressings with improved performance by impregnation with alginate. *Materials Science and Engineering: C*, 110, 110619. <https://doi.org/10.1016/j.msec.2019.110619>
  73. Sun, X., Li, R. & Xiang, J. (2025). Detection of klebsiella pneumoniae and antibiotic resistance in burn wards in china from 2019 to 2023. *Infection and Drug Resistance*, 1595-1604. <https://doi.org/10.2147/IDR.S505514>
  74. Swingler, S., Gupta, A., Gibson, H., Kowalczyk, M., Heaselgrave, W. & Radecka, I. (2021). Recent advances and applications of bacterial cellulose in biomedicine. *Polymers*, 13(3), 412. <https://doi.org/10.3390/polym13030412>
  75. Tamura, K., Stecher, G. & Kumar, S. (2021). MEGA11: molecular evolutionary genetics analysis version 11. *Molecular Biology And Evolution*, 38(7), 3022-3027. <https://doi.org/10.1093/molbev/msab120>
  76. Touaitia, R., Mairi, A., Ibrahim, N. A., Basher, N. S., Idres, T. & Touati, A. (2025). *Staphylococcus aureus*: A review of the pathogenesis and virulence mechanisms. *Antibiotics*, 14(5), 470. <https://doi.org/10.3390/antibiotics14050470>
  77. Ullah, M. W., Alabbosh, K. F., Fatima, A., Islam, S. U., Manan, S., Ul-Islam, M. & Yang, G. (2024). Advanced biotechnological applications of bacterial nanocellulose-based biopolymer nanohybrids: A review. *Advanced Industrial and Engineering Polymer Research*, 7(1), 100-121. <https://doi.org/10.1016/j.aiepr.2023.07.004>
  78. Wai Chun, C. N., Tajarudin, H. A., Ismail, N., Azahari, B. & Mohd Zaini Makhtar, M. (2021). Elucidation of mechanical, physical, chemical and thermal properties of microbial composite films by integrating sodium alginate with *Bacillus subtilis* sp. *Polymers*, 13(13), 2103. <https://doi.org/10.3390/polym13132103>
  79. Wang, C., Bai, J., Tian, P., Xie, R., Duan, Z., Lv, Q. & Tao, Y. (2021). The application status of nanoscale cellulose-based hydrogels in tissue engineering and regenerative biomedicine. *Frontiers in Bioengineering and Biotechnology*, 9, 732513. <https://doi.org/10.3389/fbioe.2021.732513>
  80. Wichai, S., Chuysinuan, P., Chairwut, S., Ekabutr, P. & Supaphol, P. (2019). Development of bacterial cellulose/alginate/chitosan composites incorporating copper (II) sulfate as an antibacterial wound dressing. *Journal of Drug Delivery Science and Technology*, 51, 662-671. <https://doi.org/10.1016/j.jddst.2019.03.043>
  81. Wu, Y., Huang, T. Y., Li, Z. X., Huang, Z. Y., Lu, Y. Q., Gao, J., ... & Huang, C. (2021). In-situ fermentation with gellan gum adding to produce bacterial cellulose from traditional Chinese medicinal herb residues hydrolysate. *Carbohydrate Polymers*, 270, 118350. <https://doi.org/10.1016/j.carbpol.2021.118350>
  82. Yang, G., Yao, Y. & Wang, C. (2017). Green synthesis of silver nanoparticles impregnated bacterial cellulose-alginate composite film with improved properties. *Materials Letters*, 209, 11-14. <https://doi.org/10.1016/j.matlet.2017.07.097>
  83. Ybañez, M. G. & Camacho, D. H. (2021). Designing hydrophobic bacterial cellulose film composites assisted by sound waves. *RSC Advances*, 11(52), 32873-32883. <https://doi.org/10.1039/D1RA02908H>
  84. Yefet, E., Schwartz, N., Chazan, B., Salim, R., Romano, S. & Nachum, Z. (2018). The safety of quinolones and fluoroquinolones in pregnancy: a meta-analysis. *BJOG: An International Journal of Obstetrics & Gynaecology*, 125(9), 1069-1076. <https://doi.org/10.1111/1471-0528.15119>